Supplementary Information for

Seamlessly merging radar ranging and imaging, wireless communications, and spectrum sensing for 6G empowered by microwave photonics

Taixia Shi[1], Yang Chen[1,*] and Jianping Yao[2,*]

*Correspondence to: Y. Chen, ychen@ce.ecnu.edu.cn; J. Yao, jpyao@uottawa.ca.

[1]Shanghai Key Laboratory of Multidimensional Information Processing, School of Communication and Electronic Engineering, East China Normal University, Shanghai, China

[2]Microwave Photonic Research Laboratory, School of Electrical Engineering and Computer Science, University of Ottawa, Ottawa, Canada

Contents

Supplementary Note 1: CS-TSSB modulation

The carrier-suppressed tandem single-sideband (CS-TSSB) modulation is used in the proposed scheme. By implementing CS-TSSB modulation at a dual-parallel Mach–Zehnder modulator (DP-MZM), a double sideband signal with an intermediate frequency (IF) ASK signal and a linearly frequency-modulated (LFM) signal located at the opposite sides of the optical carrier is generated, as shown in Supplementary Fig. 1. The principle of CS-TSSB modulation is described as follows.

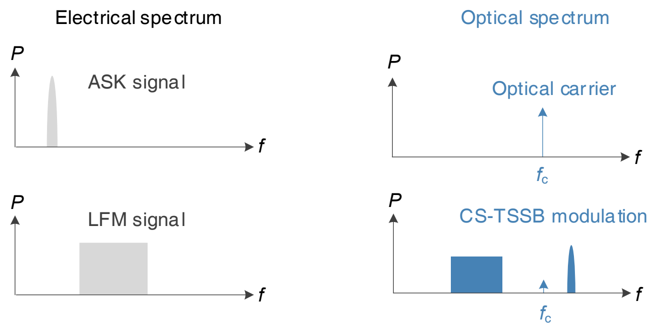

Supplementary Fig. 1 The CS-TSSB modulation. CS-TSSB, carrier-suppressed tandem single-sideband; ASK, amplitude-shift keying; LFM, linearly frequency-modulated.

It is assumed that the angular frequency of the IF ASK signal is ω_{ASK}, and the start angular frequency and chirp rate of the LFM signal are ω_{LFM} and k. The IF ASK signal and the LFM signal applied to one radio frequency (RF) port of the DP-MZM are expressed as

$$V_{\text{ASK-I}}\left(t\right) = A_{\mathrm{ASK}} \cos(\omega_{\mathrm{ASK}} t + \varphi_{\mathrm{ASK}}) , \tag{1}$$

$$V_{\text{LFM-Q}}\left(t\right) = A_{\mathrm{LFM}} \sin(\omega_{\mathrm{LFM}} t + \pi k t^2) . \tag{2}$$

where A_{LFM} and A_{ASK} are the amplitudes of the corresponding signals, and φ_{ASK} is the phase of the IF ASK signal. The IF ASK signal and the LFM signal applied to the other RF port of the DP-MZM are expressed as

$$V_{\text{ASK-Q}}\left(t\right) = A_{\mathrm{ASK}} \sin(\omega_{\mathrm{ASK}} t + \varphi_{\mathrm{ASK}}) , \tag{3}$$

$$V_{\text{LFM-I}}\left(t\right) = A_{\mathrm{LFM}} \cos(\omega_{\mathrm{LFM}} t + \pi k t^2) . \tag{4}$$

The input optical carrier of the DP-MZM is assumed to be $\exp(\mathrm{j}\omega_c t)$, where ω_c is the angular frequency of the optical carrier. The output optical signal from the DP-MZM can be expressed as

$$
\begin{aligned}
E_{\text{DP-MZM}}(t) \propto & \exp\left(\mathrm{j}\omega_{\mathrm{c}}t\right)\exp\left\{\mathrm{j}\pi\left[V_{\text{LFM-Q}}+V_{\text{ASK-I}}-V_{\pi}/2\right]\Big/V_{\pi}\right\} \\
& +\exp\left(\mathrm{j}\omega_{\mathrm{c}}t\right)\exp\left\{-\mathrm{j}\pi\left[V_{\text{LFM-Q}}+V_{\text{ASK-I}}-V_{\pi}/2\right]\Big/V_{\pi}\right\} \\
& +\exp\left(\mathrm{j}\omega_{\mathrm{c}}t-\mathrm{j}\pi/2\right)\exp\left\{\mathrm{j}\pi\left[V_{\text{LFM-I}}+V_{\text{ASK-Q}}+V_{\pi}/2\right]\Big/V_{\pi}\right\} \\
& +\exp\left(\mathrm{j}\omega_{\mathrm{c}}t-\mathrm{j}\pi/2\right)\exp\left\{-\mathrm{j}\pi\left[V_{\text{LFM-I}}+V_{\text{ASK-Q}}+V_{\pi}/2\right]\Big/V_{\pi}\right\} \\
& =2\exp\left(\mathrm{j}\omega_{\mathrm{c}}t\right)\cos\left\{\pi\left[V_{\text{LFM-Q}}+V_{\text{ASK-I}}-V_{\pi}/2\right]\Big/V_{\pi}\right\} \\
& +2\exp\left(\mathrm{j}\omega_{\mathrm{c}}t-\mathrm{j}\pi/2\right)\cos\left\{\pi\left[V_{\text{LFM-I}}+V_{\text{ASK-Q}}+V_{\pi}/2\right]\Big/V_{\pi}\right\} \\
& =2\exp\left(\mathrm{j}\omega_{\mathrm{c}}t\right)\cos\left[m_{\text{LFM}}\sin(\omega_{\text{LFM}}t+\pi kt^{2})+m_{\text{ASK}}\cos(\omega_{\text{ASK}}t+\varphi_{\text{ASK}})-\pi/2\right] \\
& -2\mathrm{j}\exp\left(\mathrm{j}\omega_{\mathrm{c}}t\right)\cos\left[m_{\text{LFM}}\cos(\omega_{\text{LFM}}t+\pi kt^{2})+m_{\text{ASK}}\sin(\omega_{\text{ASK}}t+\varphi_{\text{ASK}})+\pi/2\right] \\
& =2\exp\left(\mathrm{j}\omega_{\mathrm{c}}t\right)\sin\left[m_{\text{LFM}}\sin(\omega_{\text{LFM}}t+\pi kt^{2})+m_{\text{ASK}}\cos(\omega_{\text{ASK}}t+\varphi_{\text{ASK}})\right] \\
& +2\mathrm{j}\exp\left(\mathrm{j}\omega_{\mathrm{c}}t\right)\sin\left[m_{\text{LFM}}\cos(\omega_{\text{LFM}}t+\pi kt^{2})+m_{\text{ASK}}\sin(\omega_{\text{ASK}}t+\varphi_{\text{ASK}})\right] \\
& \approx 2\exp\left(\mathrm{j}\omega_{\mathrm{c}}t\right)\left[m_{\text{LFM}}\sin(\omega_{\text{LFM}}t+\pi kt^{2})+m_{\text{ASK}}\cos(\omega_{\text{ASK}}t+\varphi_{\text{ASK}})\right] \\
& +2\mathrm{j}\exp\left(\mathrm{j}\omega_{\mathrm{c}}t\right)\left[m_{\text{LFM}}\cos(\omega_{\text{LFM}}t+\pi kt^{2})+m_{\text{ASK}}\sin(\omega_{\text{ASK}}t+\varphi_{\text{ASK}})\right] \\
& =2m_{\text{ASK}}\exp\left(\mathrm{j}\omega_{\mathrm{c}}t+\mathrm{j}\omega_{\text{ASK}}t+\mathrm{j}\varphi_{\text{ASK}}\right) \\
& +2m_{\text{LFM}}\exp\left(\mathrm{j}\omega_{\mathrm{c}}t+\mathrm{j}\pi/2-\mathrm{j}\omega_{\text{LFM}}t-\mathrm{j}\pi kt^{2}\right).
\end{aligned}
\tag{5}
$$

In Eq. (5), V_π is the half-wave voltage of the DP-MZM, and $m_{\text{LFM}} = \pi A_{\text{LFM}}/V_\pi$ and $m_{\text{ASK}} = \pi A_{\text{ASK}}/V_\pi$ are the modulation indices. Thus, a double sideband signal with the IF ASK signal and the LFM signal located at the opposite sides of the optical carrier is obtained by the CS-TSSB modulation.

Supplementary Note 2: The amplitude unevenness of the self-mixing signal waveform

Self-mixing is used in the proposed scheme to detect the signal envelope carrying the communication data. However, because of the uneven responses of the mixer and other components in the link over a wide bandwidth, the system exhibits a greater magnitude response at lower frequencies and a smaller magnitude response at higher frequencies from 7.8 to 13.8 GHz in the main text. Therefore, the amplitude of the waveform after self-mixing is noticeably uneven and gradually increases with time.

Supplementary Fig. 2a–d shows the waveform after self-mixing when the LFM carrier of the ASK-LFM signal sweeps from 7 to 13 GHz, 6 to 12 GHz, 5 to 11 GHz, and 4 to 10 GHz, respectively. It can be seen that with the movement of the LFM carrier frequency range of the ASK-LFM signal, the unevenness of the waveform also moves with very high consistency, that is, in the four sets of experimental results, the amplitude of the waveform at any moment is determined by the frequency of the LFM carrier frequency at that moment. It should be noted that, since the negative chirped LFM signal is used in the experiment, the 0-μs moment of the waveform corresponds to the highest frequency, whereas the 4-μs moment of the waveform corresponds to the lowest frequency.

In Supplementary Fig. 2a, the amplitude of the waveform corresponding to the higher frequency band is small, which is mainly attributed to the mixer response being smaller at the higher frequency band. In Supplementary Fig. 2c and d, the amplitude of the waveform corresponding to the frequency band lower than around 5.85 GHz is very small and even has only noise components, which is mainly limited by the bandwidth of the electrical amplifier (5.85 to 14.5GHz) and the antenna operating bandwidth (8 to 18 GHz).

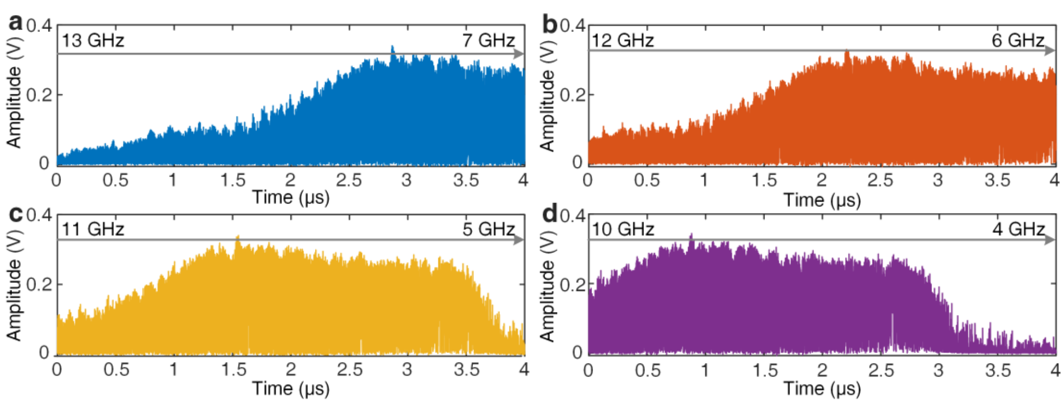

Supplementary Fig. 2 The amplitude unevenness of the waveform after self-mixing and filtering at different frequency bands, a 7 to 13 GHz, **b** 6 to 12 GHz, **c** 5 to 11 GHz, **d** 4 to 10 GHz.

After obtaining the signal envelope, further threshold setting and decision-making are required to recover the original bit information. However, due to the unevenness of the signal envelope, directly performing signal decision-making cannot correctly recover the original bit information. Therefore, compensation of the signal envelope is necessary. As indicated in Supplementary Fig. 2, it can be seen that the amplitude of the signal envelope obtained after self-mixing is closely related to the frequency of the original ASK-LFM signal that corresponds to that amplitude. Therefore, we can compensate for the uneven signal envelope by establishing the correlation between the ASK-LFM signal frequency and the amplitude of the signal envelope obtained after self-mixing in the system. This is the method we use to compensate for the uneven signal envelope in the main text.

Although a flat signal envelope can be achieved through the aforementioned method, which facilitates signal decision-making and the recovery of original bit information, an uneven signal envelope can still affect the communication performance of the system. With a fixed signal-to-noise ratio (SNR) of the received ASK-LFM signal, this will lead to a poorer SNR in the self-mixing waveform corresponding to the high-frequency band, making it more prone to bit errors, especially when the received signal power is low. As shown in Fig. 4d and e in the main text, the waveform from 3.95 to 4 μs generated by the low-frequency part of the ASK-LFM signal does have a better SNR compared to that from 0 to 0.05 μs generated by the high-frequency part of the ASK-LFM signal.

For practical applications, direct envelope detection using an envelope detector or self-mixing using a mixer with a flatter magnitude response over the wide bandwidth can mitigate the uneven amplitude of the waveform and better results can be obtained. Under these circumstances, the compensation in this work is not necessary. However, because no suitable envelope detector is available at the time of the experiment, self-mixing using a mixer is used to recover the original bit information with compensation.

Supplementary Note 3: The waveform and spectrum of the radar echo in imaging

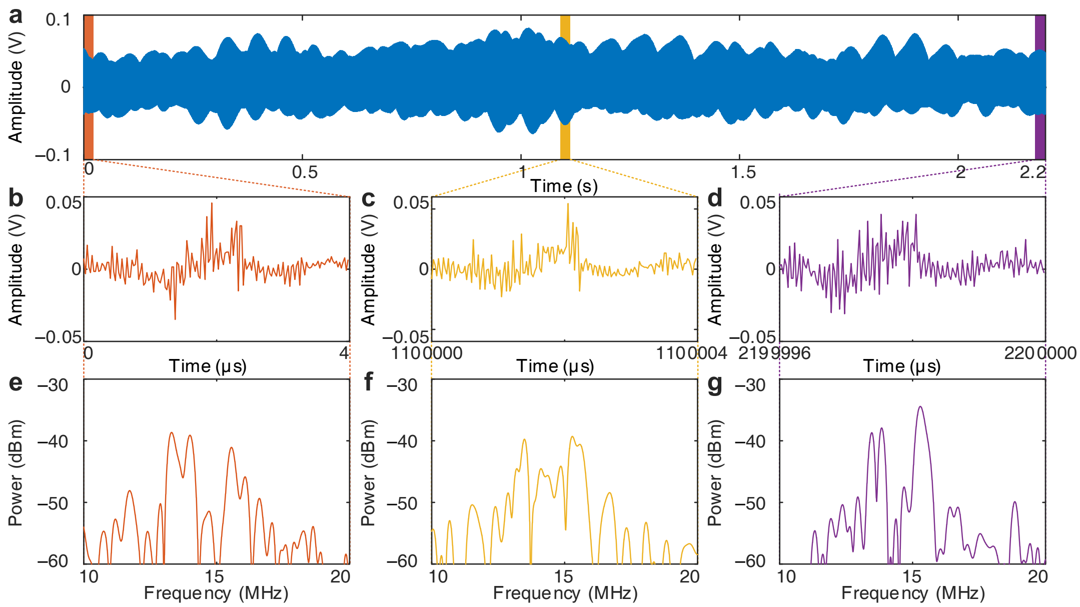

Supplementary Fig. 3 The waveform and spectrum of the radar echo. The waveform **a** in one imaging frame of 2.2 s, **b** from 0–4 μs, **c** from 1100000–1100004 μs, **d** from 2199996–2200000 μs. **e–g** are the spectra of **b–d.**

Supplementary Fig. 3a shows the waveform corresponding to the imaging result in Fig. 5d of the main text. The observed waveforms exhibit fluctuations due to variations in the radar echo signal intensity caused by the rotating imaging targets. Supplementary Fig. 3b–d shows an enlarged view of the waveform in Supplementary Fig. 3a corresponding to 0–4 μs, 1100000–1100004 μs, and 2199996–2200000 μs, respectively. Supplementary Fig. 3e–g displays the spectrum corresponding to Supplementary Fig. 3b–d. The waveforms and spectra exhibit similarities at different times, but they are not identical, due to the rotation of the imaging targets. By jointly processing the radar echo signal within 2.2 s, the imaging results shown in Fig. 5d of the main text can be obtained.

Supplementary Note 4: More spectrum sensing results

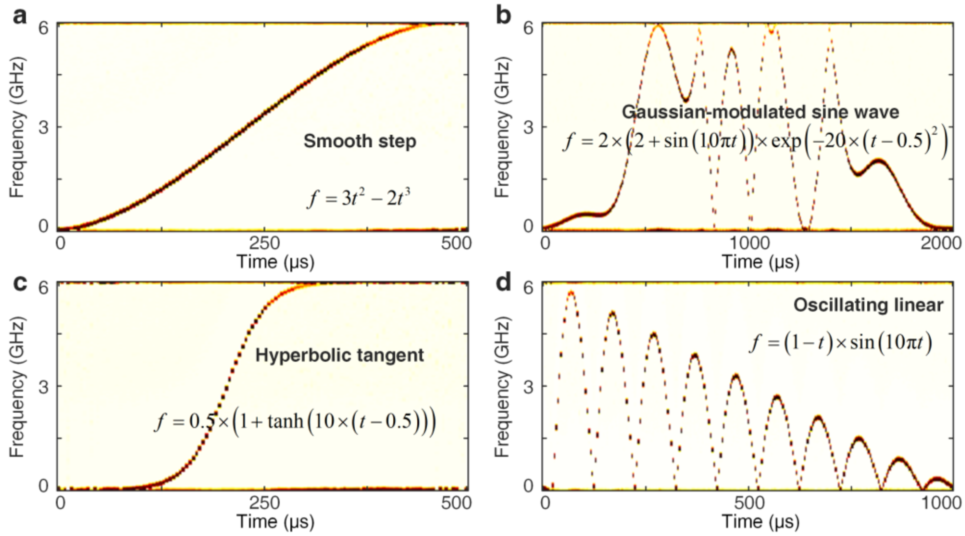

Supplementary Fig. 4 Spectrum sensing results for signals with complex time-frequency relationships.

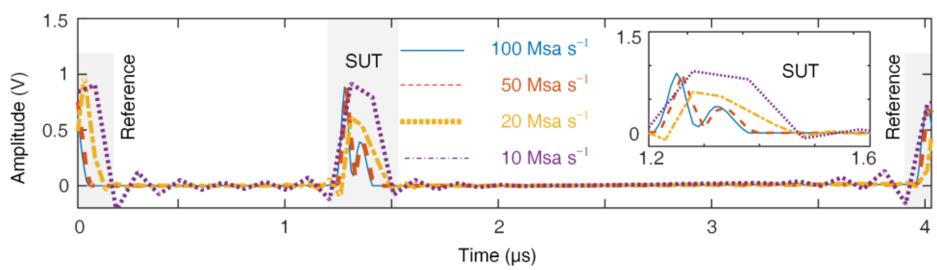

Supplementary Fig. 5 The pulse waveform from the photodetector in spectrum sensing at different sampling rates.

Supplementary Fig. 4a–d illustrates the measured two-dimensional time-frequency diagrams of signals with various time-frequency characteristics, including "smooth step", "Gaussian-modulated sine wave", "hyperbolic tangent", and "oscillating linear". It can be seen that the time-frequency diagram of a variety of signals with complex time-frequency relationships can be well recovered.

Supplementary Fig. 5 shows the generated electrical pulses in a single sweep period when a two-tone signal with frequencies of 1.92 and 2 GHz is employed. Different waveforms under different processing sampling rates are given, and each waveform corresponds to the result under the same processing sampling rate in Fig. 9e–h of the main text. The time-frequency diagram in Fig. 9e–h of the main text is a combination of pulse waveforms from multiple sweep periods, with one representative period of waveform depicted in Supplementary Fig. 5. The impact of the sampling rate on frequency resolution can be observed. It is evident that the pulses for the two tones can be distinguished when the sampling rate is 100 MSa s^{-1} or 50 MSa s^{-1}. Nevertheless, when the sampling rate is further reduced to 20 MSa s^{-1} and 10 MSa s^{-1}, the pulses for the two tones become indistinguishable.